



Active vibration control of structure by Active Mass Damper and Multi-Modal Negative Acceleration Feedback control algorithm



Don-Ho Yang^a, Ji-Hwan Shin^a, HyunWook Lee^b, Seoug-Ki Kim^a,
Moon K. Kwak^{a,*}

^a Department of Mechanical, Robotics and Energy Engineering, Dongguk University-Seoul, 30 Pildong-ro 1gil, Jung-gu, Seoul 04620, Republic of Korea

^b ICT-Railroad Convergence Research Team, New Transportation Systems Research Center, Korea Railroad Research Institute, 176 Cheoldo Bangmulgwan-ro, Uiwang-si, Gyeonggi-do 16105, Republic of Korea

ARTICLE INFO

Article history:

Received 28 July 2016

Received in revised form

20 December 2016

Accepted 21 December 2016

Available online 26 December 2016

Keywords:

Multi-modal negative acceleration feedback
Active mass damper
Active vibration control

ABSTRACT

In this study, an Active Mass Damper (AMD) consisting of an AC servo motor, a movable mass connected to the AC servo motor by a ball-screw mechanism, and an accelerometer as a sensor for vibration measurement were considered. Considering the capability of the AC servo motor which can follow the desired displacement accurately, the Negative Acceleration Feedback (NAF) control algorithm which uses the acceleration signal directly and produces the desired displacement for the active mass was proposed. The effectiveness of the NAF control was proved theoretically using a single-degree-of-freedom (SDOF) system. It was found that the stability condition for the NAF control is static and it can effectively increase the damping of the target natural mode without causing instability in the low frequency region. Based on the theoretical results of the SDOF system, the Multi-Modal NAF (MMNAF) control is proposed to suppress the many natural modes of multi-degree-of-freedom (MDOF) systems using a single AMD. It was proved both theoretically and experimentally that the MMNAF control can suppress vibrations of the MDOF system.

© 2016 Elsevier Ltd. All rights reserved.

1. Introduction

The reduction of vibrations in structures is a main engineering objective for human, machineries, sensitive instruments, automobiles, airplanes and buildings since excessive vibrations may harm the human body and cause structural failure. To this end, many new devices and control algorithms have been proposed. All of these devices and control algorithms have both advantages and disadvantages. In some cases, structural modification may not be possible and an auxiliary system which can absorb the vibration of the main structure is preferred. A Tuned Mass Damper (TMD) which can be easily attached to the structure of interest was developed to suppress the vibration of the primary structure. The TMD is a passive system that suppresses the vibration of the primary structure by tuning its natural frequency to the excitation frequency [1]. However, the TMD has limited performance due to fixed damper parameters, a narrow suppression frequency range, ineffective reduction of non-stationary vibration, and a sensitivity problem because of detuning.

* Corresponding author.

E-mail address: kwakm@dongguk.edu (M.K. Kwak).

In order to overcome the limitations of the traditional TMD, the Semi-active Tuned Mass Damper (STMD) and the Active Tuned Mass Damper (ATMD) or the Active Mass Damper (AMD) were proposed. Both technologies utilize the electronic circuit and control board to sense the motion of structure and to activate the control force. However, the STMD does not produce a direct force but rather changes its natural frequency by changing either stiffness or damping properties to suppress vibrations. This is advantageous compared to the AMD when the electrical power is not available since it can still provide existing damping or stiffness to structure. The AMD applies a control force computed by using a sensor signal and control algorithm, thus resulting in active vibration control. The AMD is capable of suppressing vibrations due to the frequently varying external environment since it uses actuators, sensors, and a feedback control algorithm. However, it may destabilize a main structure if structural parameters change. Hence, the reliability of the control system should be guaranteed before implementation.

Hrovat et al. [2] proposed a STMD consisting of a control-valve actuator and a Linear Quadratic Regulator (LQR). Pinkaew and Fujino [3] investigated a STMD that uses variable damping under harmonic excitation and also used a LQR. Lin and Chung [4] employed the magneto-rheological (MR) damper and developed a clipped optimal control, which compares the state-output-feedback LQR control force and the estimated MR damper force. Varadarajan and Nagarajaiah [5], Nagarajaiah and Vardarajan [6], Nagarajaiah and Sonmez [7], Lin et al. [8], and Kwak et al. [9] proposed a STMD which can adjust the modulus of stiffness thus tuning to the changing excitation frequency.

Chung et al. [10] proposed control algorithms for the active tendon control of seismic structures based on instantaneous optimal control. Kobori et al. [11,12] proposed the design method of the active mass driver system and simplified the control algorithm obtained by applying the optimal control theory. Chang and Yang [13] studied the AMD using velocity feedback and a complete feedback control that utilizes displacement, velocity and acceleration measurements. Ankireddi and Yang [14] investigated the AMD using complete feedback control. Cao et al. [15] applied the AMD to a tall TV tower using the Linear Quadratic Regulator (LQR) and a nonlinear feedback control algorithm. Baoya and Chunxiang [16] developed a robust control algorithm for the AMD. Samali and Al-Dawod [17] applied the Fuzzy logic controller to the AMD. Cao and Li [18] proposed new control strategies for the AMD. Wang and Lin [19] developed the variable structure control and Fuzzy sliding mode control for the AMD. The AMD has been successfully applied to skyscrapers to cope with earthquake and wind excitations.

Research on control algorithms for the AMD mentioned above assumed that the displacement, velocity and acceleration are measurable. However, it is difficult to directly measure the displacement and velocity of a real vibrating structure since the most popular sensor for vibration measurement is an accelerometer. The displacement and velocity can be thought to be obtainable by integrating the acceleration signal. However, bias and drift involved in the acceleration signal may cause problems in the integration process. Hence, researchers have proposed the direct use of the acceleration signal to produce a proper control action.

Dyke et al. [20] showed that H2/LQG frequency domain control methods employing acceleration feedback can be effectively used for the vibration suppression of seismic structures. Nishimura et al. [21,22] developed a feedback control algorithm using acceleration. Dyke et al. [23] developed a state feedback control algorithm using acceleration as the sensor output. Sim and Lee [24] proposed the acceleration feedback control and proved its stability. Christenson et al. [25] proposed the active coupled building control using acceleration feedback and used the H2/LQG approach to obtain the control algorithm. Mahmoodi, et al. [26] proposed the modified acceleration feedback control for collocated piezoelectric actuators and accelerometer. Enrizuea-Zarate et al. [27] proposed the positive acceleration feedback control when one beam-column of a building-like structure is coupled with a PZT stack actuator. These controllers are more realistic than the other controllers mentioned above because they use acceleration to generate the control signal for piezoelectric actuators. However, the above studies did not deal with the AMD actuated by an AC servo motor that can provide accurate position tracking rather than control force.

This study is concerned with the AMD actuated by the AC servo motor and a ball-screw mechanism, which appears to be the most feasible mechanism for the real application of AMD when the target natural frequency is low. Also, the proposed AMD system doesn't require high-voltage power source to activate large control force. Watanabe et al. [28] proposed the LQ control combined with a low-pass filter for the active vibration control of high-rise buildings but their algorithm requires complicated computations. The advantage of our mechanism is that the movement of the active mass can be accurately controlled by the AC servo motor. In general, the AC servo motor is operated with either the position, velocity or torque modes. The rotation of the AC servo motor is accurately controlled by the internal PID controller according to the input command. The sensor for the proposed AMD is of course an accelerometer for practical purposes. Hence, a control algorithm that utilizes acceleration and produces the desired position of the active mass needs to be developed. To this end, the Negative Acceleration Feedback (NAF) control is proposed for the proposed AMD system. The proposed NAF control is different from other control algorithms that produce control force. Also, the NAF control theory that directly uses accelerometer signal as a sensor input is different from other control theories that require displacement or velocity. The effectiveness of the NAF control was first investigated by applying it to the single-degree-of-freedom (SDOF) system. The Routh-Hurwitz method was employed to examine the stability of the NAF control. It was theoretically determined that the stability condition is static. The Multi-Modal NAF (MMNAF) control was then developed to increase the damping of the many natural modes of a multi-degree-of-freedom (MDOF) system using a single AMD. Theoretical result shows that the proposed multi-modal NAF control can be successfully applied to the MDOF system if the gain matrix is sufficiently small. The test bed was built to examine the performance of the proposed MMNAF control. Experimental results show that the MMNAF control can successfully suppress vibrations in the structure.

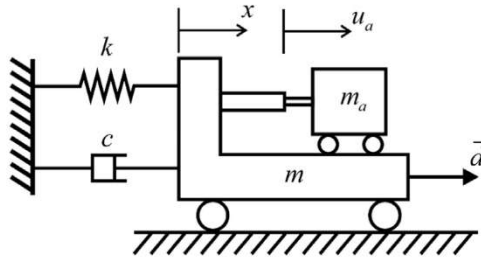


Fig. 1. Schematic diagram for single-degree-of-freedom.

2. Negative acceleration feedback control for active mass damper

Fig. 1 shows a SDOF model equipped with the AMD. It is assumed that the displacement of the actuator such as a ball-screw mechanism or linear motor is used to accurately control the position of the movable mass. m , c , k are the mass, damping, and spring constant of the primary system and m_a is the mass of the movable mass. x is the displacement of the primary mass and u_a is the relative displacement of the additional mass with respect to the primary mass. \bar{d} is the external disturbance acting on the primary mass.

The equation of motion for this system can be written as follows:

$$(m + m_a)\ddot{x} + c\dot{x} + kx = -m_a\ddot{u}_a + \bar{d} \quad (1)$$

Dividing the equation of motion by $m + m_a$ and introducing non-dimensional constants and variables, Eq. (1) can be rewritten as

$$\ddot{x} + 2\zeta\omega_n\dot{x} + \omega_n^2x = -g\ddot{u} + \omega_n^2d \quad (2)$$

where g is the gain for the control

$$\omega_n = \sqrt{\frac{k}{m + m_a}}, \quad \zeta = \frac{c}{2(m + m_a)\omega_n}, \quad u = \frac{m_a}{g(m + m_a)}u_a, \quad d = \frac{\bar{d}}{k} \quad (3a-d)$$

In this study, we propose the Negative Acceleration Feedback (NAF) controller expressed by the following equation.

$$\ddot{u} + 2\zeta_c\omega_n\dot{u} + \omega_n^2u = -g\ddot{x} \quad (4)$$

where ζ_c is the damping factor for the controller. In practice, an accelerometer is a popular sensor for vibration measurement. Hence, the implementation of the control algorithm given by Eq. (4) can be realized by the following simple transfer function if the accelerometer is used as a sensor.

$$\frac{U}{\ddot{X}} = -\frac{g}{s^2 + 2\zeta_c\omega_n s + \omega_n^2} \quad (5)$$

Eq. (5) implies that the desired position for the movable mass can be determined by the acceleration of the primary mass. The transfer function of the control law is in fact a low-pass filter. The controller taking the form of a low-pass filter has been used in the vibration suppression of structures using piezoelectric sensors and actuators, which is called the Positive Position Feedback (PPF) control [29]. The PPF control implies that it utilizes the position sensor and positive feedback loop. However, the controller proposed in this study is the NAF control as shown in Eq. (5) and its output is the displacement of the active mass. The bode plot for the transfer function given by Eq. (5) is shown in Fig. 2. $g = 0.3$, $\omega_n = 1$ rad/s are used. It can be seen from Fig. 2 that the NAF control has peak magnitude at the filter frequency and 90 degree phase shift similar to the PPF control.

Let us investigate the stability of the NAF proposed in this study. By applying the Laplace transform to Eqs. (2) and (4), we can obtain

$$\begin{aligned} (s^2 + 2\zeta\omega_n s + \omega_n^2)X + gs^2U &= D \\ gs^2X + (s^2 + 2\zeta_c\omega_n s + \omega_n^2)U &= 0 \end{aligned} \quad (6)$$

In matrix form, we can obtain

$$\begin{bmatrix} s^2 + 2\zeta\omega_n s + \omega_n^2 & gs^2 \\ gs^2 & s^2 + 2\zeta_c\omega_n s + \omega_n^2 \end{bmatrix} \begin{Bmatrix} X \\ U \end{Bmatrix} = \begin{Bmatrix} D \\ 0 \end{Bmatrix} \quad (7)$$

Therefore, the transfer function between the disturbance and the displacement of the primary mass can be derived as

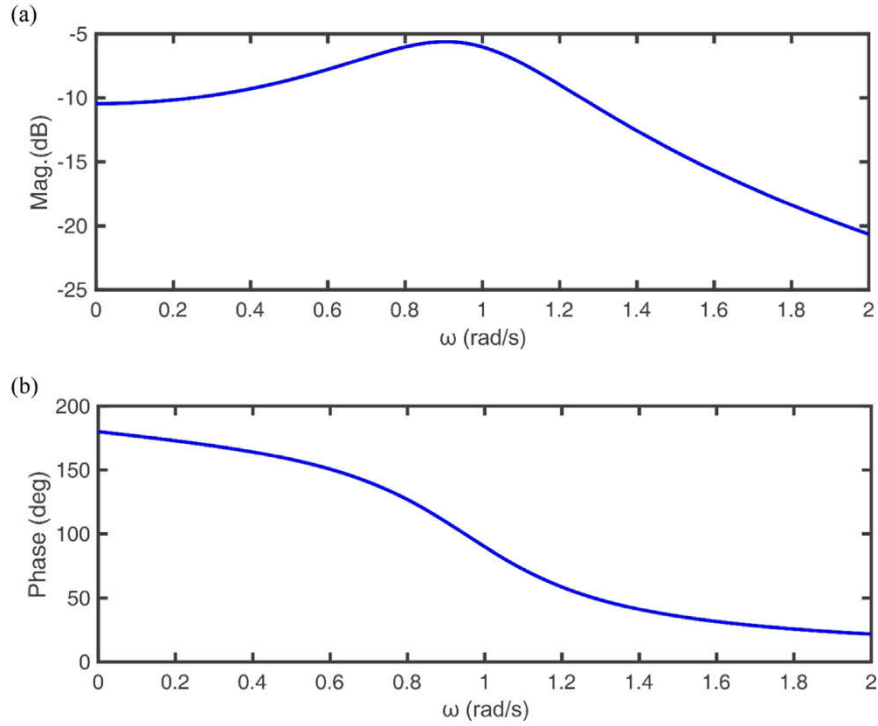


Fig. 2. Bode plot for NAF control: (a) Magnitude, (b) Phase.

$$\frac{X}{D} = \frac{(s^2 + 2\zeta_c \omega_n s + \omega_n^2)\omega_n^2}{(1 - g^2)s^4 + 2(\zeta + \zeta_c)\omega_n s^3 + 2(1 + 2\zeta\zeta_c)\omega_n^2 s^2 + 2(\zeta + \zeta_c)\omega_n^3 s + \omega_n^4} \quad (8)$$

From Eq. (8), the denominator is

$$\text{den}(s) = (1 - g^2)s^4 + 2(\zeta + \zeta_c)\omega_n s^3 + 2(1 + 2\zeta\zeta_c)\omega_n^2 s^2 + 2(\zeta + \zeta_c)\omega_n^3 s + \omega_n^4 \quad (9)$$

By applying the Routh-Hurwitz criteria, the following stability condition can be obtained.

$$\text{stable if } 0 < g < 1 \quad (10)$$

It can be readily seen that the above stability condition is static, which implies that the stability of the closed-loop system does not depend on the frequency. Let us investigate the effect of the NAF control on the resonant amplitude. By applying $s = i\omega_n$ to Eq. (8) and deriving the magnitude, we can obtain

$$\left| \frac{X}{D} \right|_{s=i\omega_n} = \frac{1}{2\left(\zeta + \frac{g^2}{4\zeta_c}\right)} \quad (11)$$

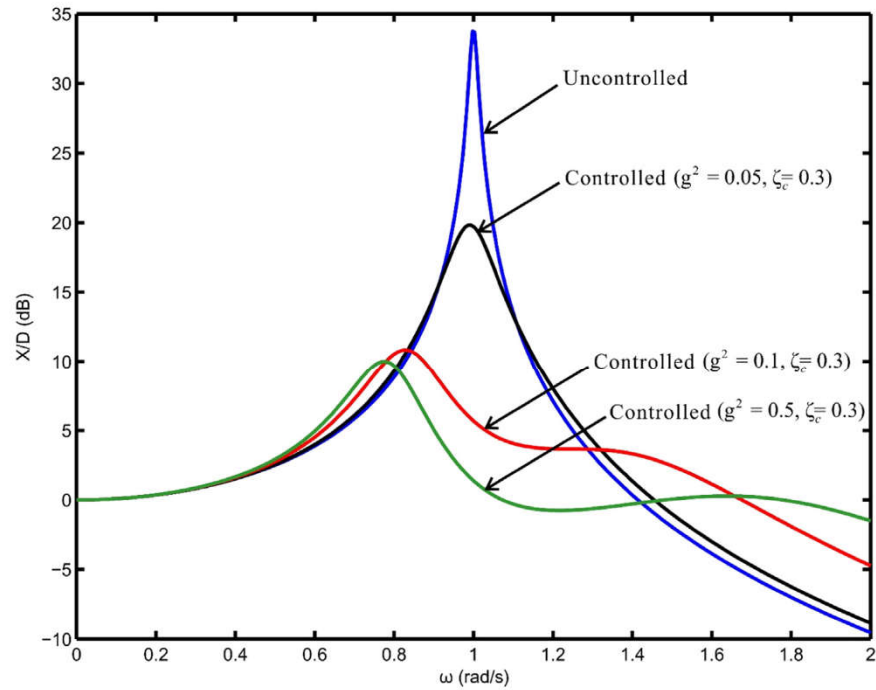
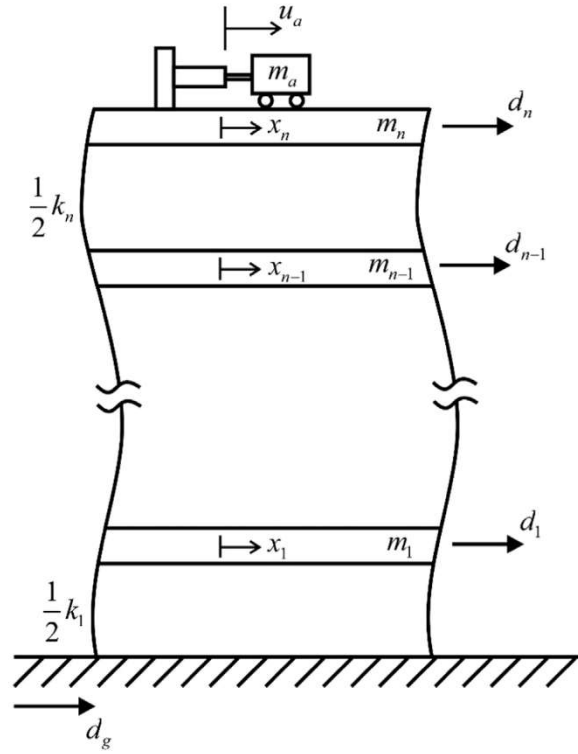
It can be readily seen from Eq. (11) that the active damping can be achieved by choosing a proper gain and damping factor for the controller. Like the PPF control, it seems practical to use 0.3 for ζ_c . If we use 0.3 for ζ_c and g^2 , then the active damping increases by 0.25. Fig. 3 shows the frequency response plot for the SDOF system. $\omega_n = 1$ rad/s, $\zeta = 0.01$, $\zeta_c = 0.3$ are used for this figure. Unlike the PPF control, static instability does not appear as the gain increases.

3. Multi-modal negative acceleration feedback control

Let us consider a MDOF system that is an n -story building with an AMD at the top as shown in Fig. 4. The equations of motion for this system can be written as

$$\mathbf{M}\ddot{\mathbf{x}} + \mathbf{C}\dot{\mathbf{x}} + \mathbf{K}\mathbf{x} = -\mathbf{B}_a\ddot{u}_a + \mathbf{d} \quad (12)$$

where $\mathbf{x} = [x_1 \ x_2 \ \dots \ x_n]^T$ and

**Fig. 3.** Frequency response plot for the SDOF system.**Fig. 4.** Schematic diagram for multi-degree-of-freedom with AMD.

$$\mathbf{M} = \begin{bmatrix} m_1 & 0 & \cdots & 0 \\ 0 & m_2 & \cdots & 0 \\ \vdots & \vdots & \ddots & \vdots \\ 0 & 0 & \cdots & m_n \end{bmatrix}, \quad \mathbf{C} = \begin{bmatrix} c_1 + c_2 & -c_2 & \cdots & 0 \\ -c_2 & c_2 + c_3 & \cdots & 0 \\ \vdots & \vdots & \ddots & \vdots \\ 0 & 0 & \cdots & c_n \end{bmatrix}, \quad (13a, b)$$

$$\mathbf{K} = \begin{bmatrix} k_1 + k_2 & -k_2 & \cdots & 0 \\ -k_2 & k_2 + k_3 & \cdots & 0 \\ \vdots & \vdots & \ddots & \vdots \\ 0 & 0 & \cdots & k_n \end{bmatrix}, \quad \mathbf{B}_a = \begin{bmatrix} 0 \\ 0 \\ \vdots \\ m_a \end{bmatrix}, \quad d = \left\{ \begin{array}{l} d_1 - m_1 \ddot{d}_g \\ d_2 - m_2 \ddot{d}_g \\ \vdots \\ d_n - (m_n + m_a) \ddot{d}_g \end{array} \right\} \quad (13c-e)$$

in which m_i , c_i , k_i ($i = 1, 2, \dots, n$) are the mass, damping, and spring constant of i^{th} floor. m_a is the active mass, d_i ($i = 1, 2, \dots, n$) is the disturbance acting on the i^{th} floor and d_g represents the ground motion. The free vibration problem results in the following eigenvalue problem.

$$(\mathbf{K} - \omega^2 \mathbf{M}) \mathbf{A} = 0 \quad (14)$$

By solving the eigenvalue problem, we can obtain the eigenvector matrix \mathbf{U} , which satisfies the orthonormality condition.

$$\mathbf{U}^T \mathbf{M} \mathbf{U} = \mathbf{I}, \quad \mathbf{U}^T \mathbf{K} \mathbf{U} = \Lambda \quad (15a, b)$$

where \mathbf{I} is an $n \times n$ identity matrix,

$$\Lambda = \begin{bmatrix} \omega_1^2 & 0 & \cdots & 0 \\ 0 & \omega_2^2 & \cdots & 0 \\ \vdots & \vdots & \ddots & \vdots \\ 0 & 0 & \vdots & \omega_n^2 \end{bmatrix} \quad (16)$$

in which ω_i ($i = 1, 2, \dots, n$) is the i^{th} natural frequency. If we apply the modal transformation, $\mathbf{x} = \mathbf{U}\mathbf{q}$, into Eq. (12) and use the orthonormality condition given by Eq. (15), then we can obtain the modal equations of motion.

$$\ddot{\mathbf{q}} + 2\mathbf{Z}\Omega\dot{\mathbf{q}} + \Lambda\mathbf{q} = -\bar{\mathbf{B}}_a \ddot{u}_a + \bar{\mathbf{d}} \quad (17)$$

where $\bar{\mathbf{B}}_a = \mathbf{U}^T \mathbf{B}_a$, $\bar{\mathbf{d}} = \mathbf{U}^T \mathbf{d}$ and

$$\Omega = \begin{bmatrix} \omega_1 & 0 & \cdots & 0 \\ 0 & \omega_2 & \cdots & 0 \\ \vdots & \vdots & \ddots & \vdots \\ 0 & 0 & \vdots & \omega_n \end{bmatrix}, \quad \mathbf{Z} = \begin{bmatrix} \zeta_1 & 0 & \cdots & 0 \\ 0 & \zeta_2 & \cdots & 0 \\ \vdots & \vdots & \ddots & \vdots \\ 0 & 0 & \vdots & \zeta_n \end{bmatrix} \quad (18a, b)$$

In deriving Eq. (17), modal damping was assumed.

In reality, there are more natural modes than available sensors and it is not desirable to control all modes with a single AMD. Of course, we can install more AMDs to control many modes but this is not economical. Let us consider a case of controlling some modes with a single AMD. In this case, it is assumed that the control force can be represented by

$$\mathbf{GQ} = \bar{\mathbf{B}}_{ac} u_a \quad (19)$$

where \mathbf{Q} is an $n_c \times 1$ modal control force vector, \mathbf{G} is an $n_c \times n_c$ diagonal matrix whose diagonals are the gain for each mode, and n_c is the number of natural modes to be controlled. $\bar{\mathbf{B}}_{ac}$ is the submatrix of $\bar{\mathbf{B}}_a$ which is obtained by considering the natural modes to be controlled. Hence, we may write $\bar{\mathbf{B}}_a = [\bar{\mathbf{B}}_{ac}^T \quad \bar{\mathbf{B}}_{au}^T]^T$. The pseudo-inverse technique is used for the solution of Eq. (19). Then, we may write

$$u_a = \bar{\mathbf{B}}_{ac}^+ \mathbf{GQ} \quad (20)$$

where $\bar{\mathbf{B}}_{ac}^+$ is the pseudo-inverse of $\bar{\mathbf{B}}_{ac}$. Inserting Eq. (20) into Eq. (17), we can obtain

$$\ddot{\mathbf{q}} + 2\mathbf{Z}\Omega\dot{\mathbf{q}} + \Lambda\mathbf{q} = -\bar{\mathbf{B}}_a \bar{\mathbf{B}}_{ac}^+ \mathbf{GQ} + \Lambda\bar{\mathbf{d}} \quad (21)$$

The Multi-Modal NAF control for Eq. (21) can then be designed as

$$\ddot{\mathbf{Q}} + 2\mathbf{Z}_c \Omega_c \dot{\mathbf{Q}} + \Lambda_c \mathbf{Q} = -\mathbf{G} (\bar{\mathbf{B}}_a \bar{\mathbf{B}}_{ac}^+)^T \ddot{\mathbf{q}} \quad (22)$$

where \mathbf{Z}_c is the damping matrix for the NAF control. Combining Eqs. (21) and (22), we can obtain

Table 1

Parameters for numerical simulation.

Parameters	Numerical values
Number of stories	40
Height of building	200m
Width of building	40m
Mass of each floor	$8 \times 10^5 \text{ kg}$
Stiffness of each floor	1.35GN/m
Damping coefficient	$\zeta = 0.01$
Mass of movable mass	10^5 kg

$$\begin{bmatrix} \mathbf{I}_{n \times n} & \bar{\mathbf{B}}_a \bar{\mathbf{B}}_{ac}^\dagger \mathbf{G} \\ \mathbf{G} (\bar{\mathbf{B}}_a \bar{\mathbf{B}}_{ac}^\dagger)^T & \mathbf{I}_{n_c \times n_c} \end{bmatrix} \begin{Bmatrix} \ddot{\mathbf{q}} \\ \ddot{\mathbf{Q}} \end{Bmatrix} + \begin{bmatrix} 2Z\Omega & \mathbf{0}_{n \times n_c} \\ \mathbf{0}_{n_c \times n} & 2Z_c\Omega_c \end{bmatrix} \begin{Bmatrix} \dot{\mathbf{q}} \\ \dot{\mathbf{Q}} \end{Bmatrix} + \begin{bmatrix} \Lambda & \mathbf{0}_{n \times n_c} \\ \mathbf{0}_{n_c \times n} & \Lambda_c \end{bmatrix} \begin{Bmatrix} \mathbf{q} \\ \mathbf{Q} \end{Bmatrix} = \begin{Bmatrix} \bar{\mathbf{d}} \\ \mathbf{0}_{n_c \times 1} \end{Bmatrix} \quad (23)$$

Hence, the stability condition can be obtained as

$$\text{stable if } \mathbf{I} - \bar{\mathbf{B}}_a \bar{\mathbf{B}}_{ac}^\dagger \mathbf{G}^2 (\bar{\mathbf{B}}_a \bar{\mathbf{B}}_{ac}^\dagger)^T > 0 \quad (24)$$

If the gain matrix is sufficiently small, then the closed-loop system is stable.

4. Numerical simulation

Numerical simulation was carried out to investigate the performance of the MMNAF control proposed in this study. The building model employed for the simulation has forty floors with 40 m width and 200 m height. Parameters for the building model are listed in Table 1. It was assumed that the base was excited by an earthquake and the El Centro earthquake data shown in Fig. 5 was used. The natural frequencies for the building were found to be 0.25, 0.76, 1.27, 1.77, and 2.27 Hz. The MMNAF controller which can tackle the first and second natural modes was designed. The following gain matrix was used

$$\mathbf{G} = \begin{bmatrix} 0.4 & 0 \\ 0 & 0.15 \end{bmatrix}$$

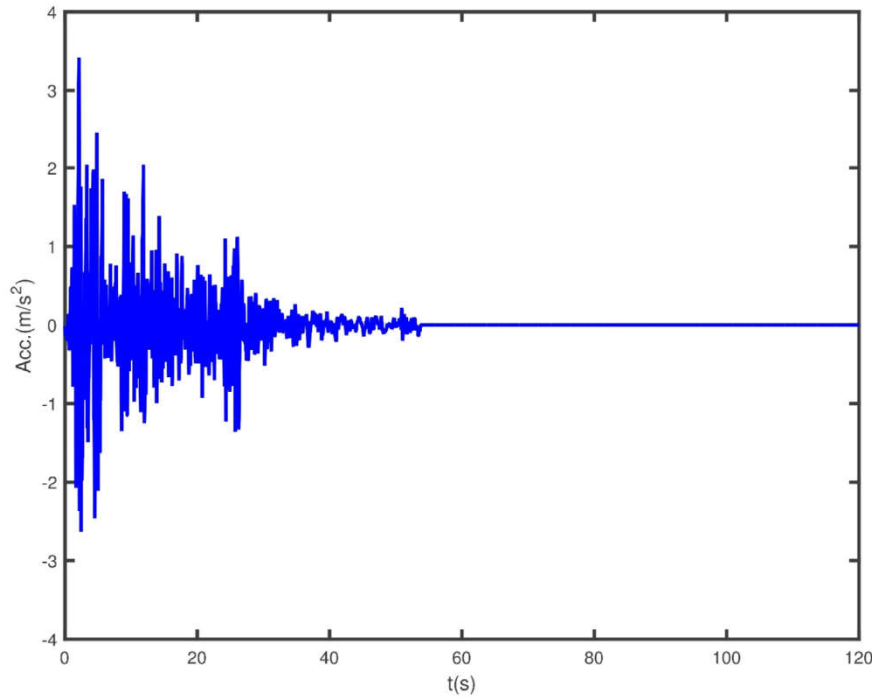


Fig. 5. Time history of acceleration for the El Centro earthquake.

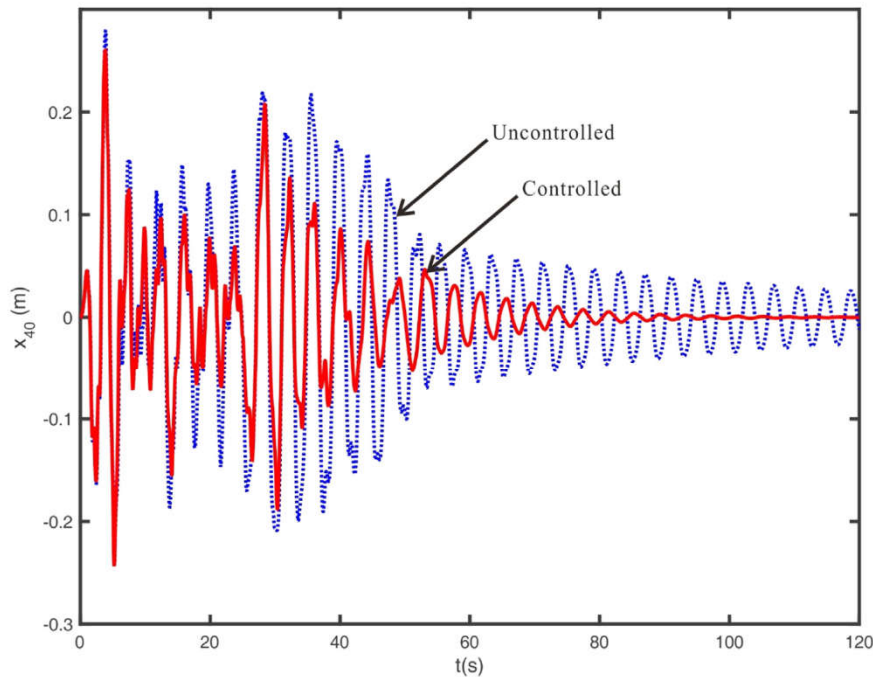


Fig. 6. Time history of top displacement for the building with and without control.

The displacements at the fortieth floor with and without MMNAF control are shown in Fig. 6. Even though the peak amplitude caused by the earthquake cannot be reduced by the MMNAF control, the response decreases rapidly by the introduction of the MMNAF control. Fig. 6 confirms that the building vibrations can be controlled by the proposed MMNAF control. Fig. 7 shows the displacement of the active mass to achieve the control performance and the maximum stroke for the control is found to be about ± 2 m. Fig. 8 shows the Frequency Response Function (FRF) for the top displacement of the building with and without control. It can be seen from Fig. 8 that the resonant amplitudes of the first and second natural modes are reduced by the MMNAF control.

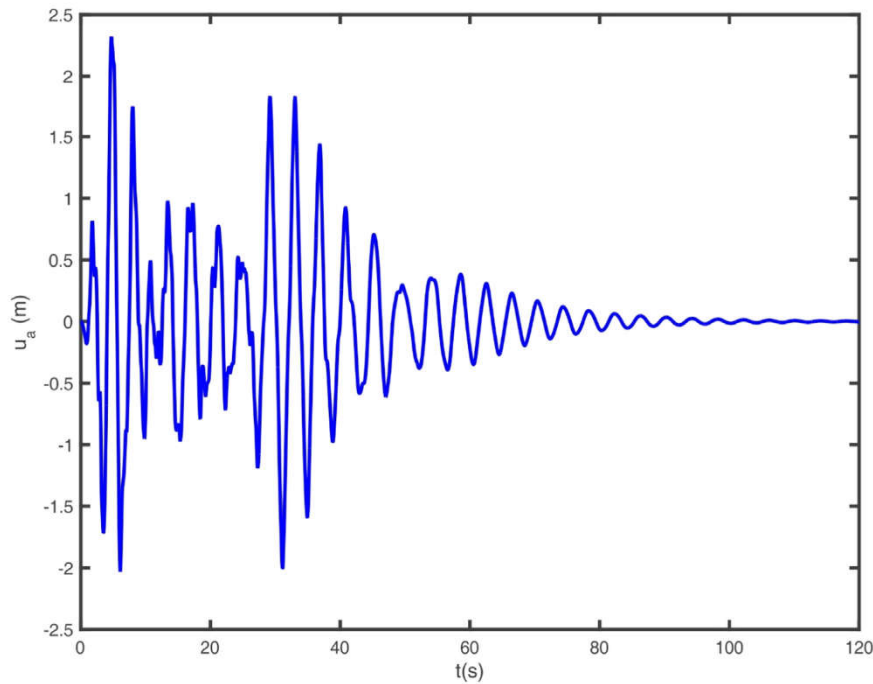


Fig. 7. Time history of active mass displacement.

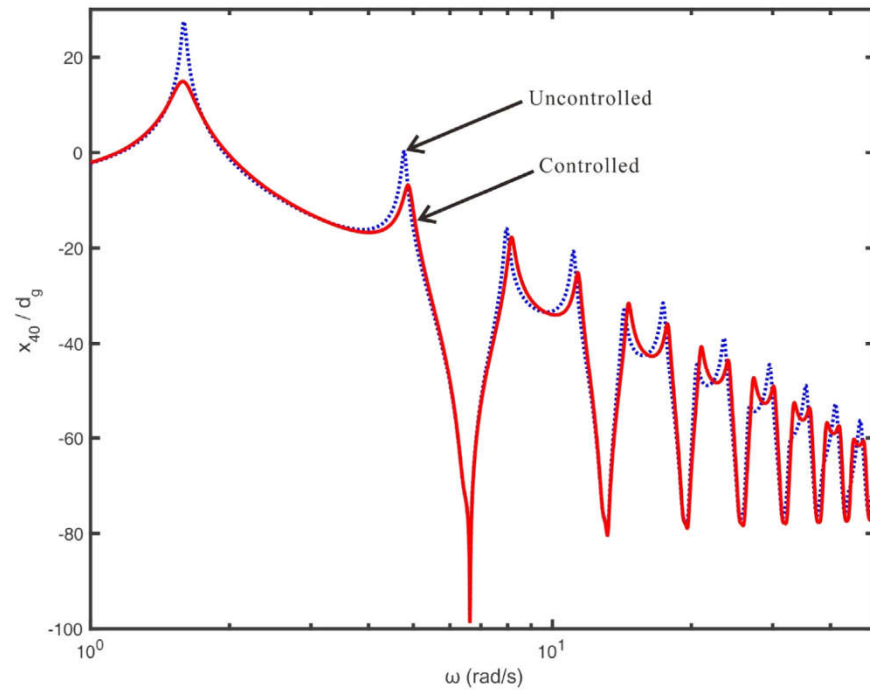


Fig. 8. FRF of top displacement for the building with and without control.

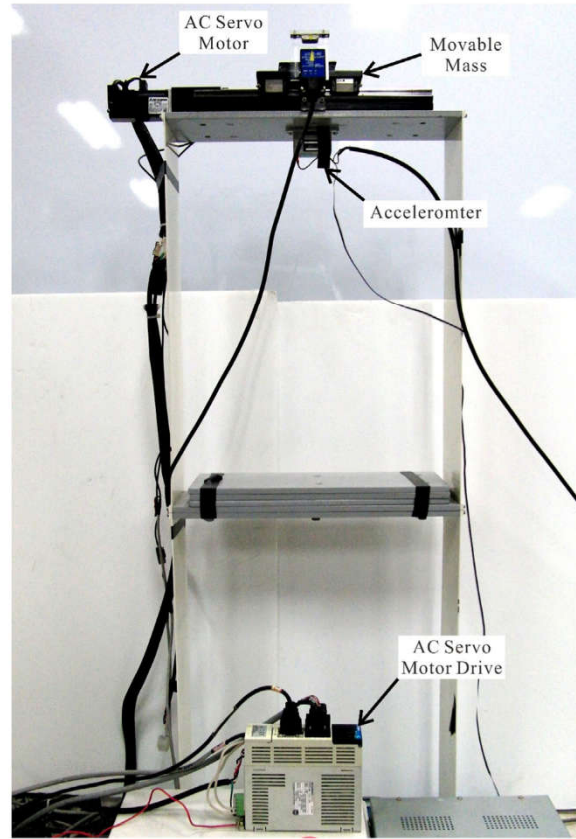
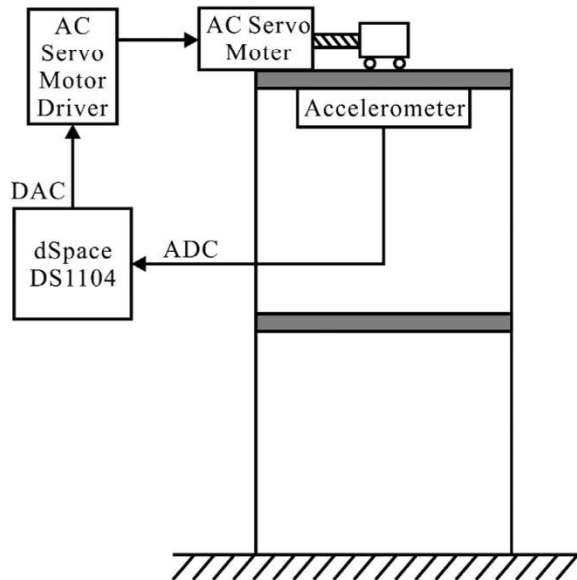


Fig. 9. Test bed for MMNAF control experiment.

Table 2

Parameters of test bed.

parameters	Numerical values
Number of stories	2
Height of test bed	1.15 m
Width of test bed	0.4m
Mass of top floor	6.9kg
Mass of middle floor	20kg
Damping coefficient of test bed	$\zeta = 0.0063$

**Fig. 10.** Schematic diagram for experimental set up.

It can be concluded from the numerical simulation that the MMNAF control can suppress the vibrations of the MDOF system.

5. Experiments

To validate the MMNAF control proposed in this study, the test bed was built as shown in Fig. 9. The test bed consists of two floors and the active mass is connected to the AC servo motor by the ball-screw mechanism. The parameters of the test bed are summarized in Table 2. The first and second natural frequencies for the test bed were found to be 0.95 Hz and 2.70 Hz, respectively. They were measured experimentally.

The AC servo motor, Mitsubishi HC-KFS13 [30] and a servomotor driver, Mitsubishi MR-J2S-10A [31], were used. The active mass was mounted on the linear motion guide. The ball-screw had a pitch of 5 mm. The vibration at the top was measured by the accelerometer, LCF-200-0.5 g from Jewell Instruments [32]. The sensitivity of this sensor was 10 V/g. Fig. 10 shows the connection diagram for the test bed.

The accelerometer signal was fed into the ADC terminals of the DS 1104 controller from dSpace Inc. [33]. Although the MMNAF controller given by Eqs. (20) and (22) compute the desired displacement of the movable mass, it was found that the real-time tracking control of the desired position of the movable mass by the AC servomotor was not possible using the position command mode of the AC servomotor driver. Hence, the velocity command mode that accepts analog signal was used instead, so that the additional PID controller was introduced as shown in Fig. 11(a). The PID controller was designed to provide proper velocity command to reduce the error between the desired position and the measured position. Also, the internal PID controller of the AC servomotor driver was utilized to follow the desired velocity as shown in Fig. 11(b). The MMNAF control algorithm and the AC servomotor control algorithm were built using the Simulink software shown in Fig. 11. The MMNAF controller consists of two NAF controllers. Each NAF controller was tuned to the first and second natural frequencies. The gains for each NAF controller were 1 and 0.1, which were determined experimentally.

Fig. 12 shows the time history of acceleration when the first natural mode of the structure was excited. As can be seen from Fig. 12(b), the MMNAF control is effective in suppressing the first natural mode. Fig. 13 shows the time history of acceleration

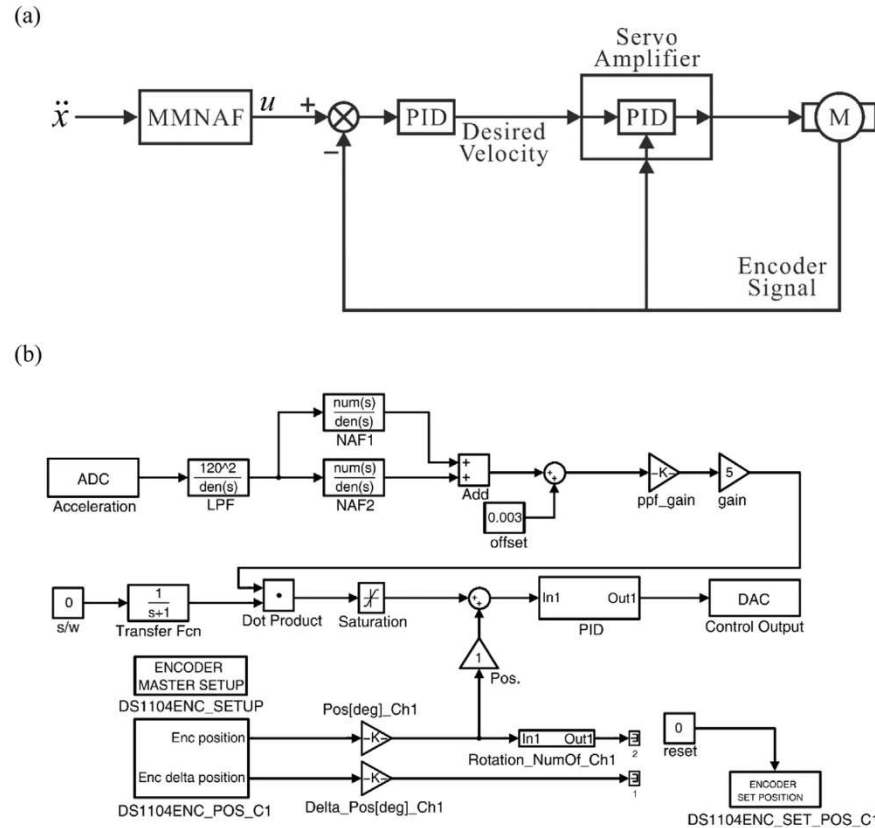


Fig. 11. Control Scheme of MMNAF control: (a) Schematic diagram, (b) Simulink block diagram.

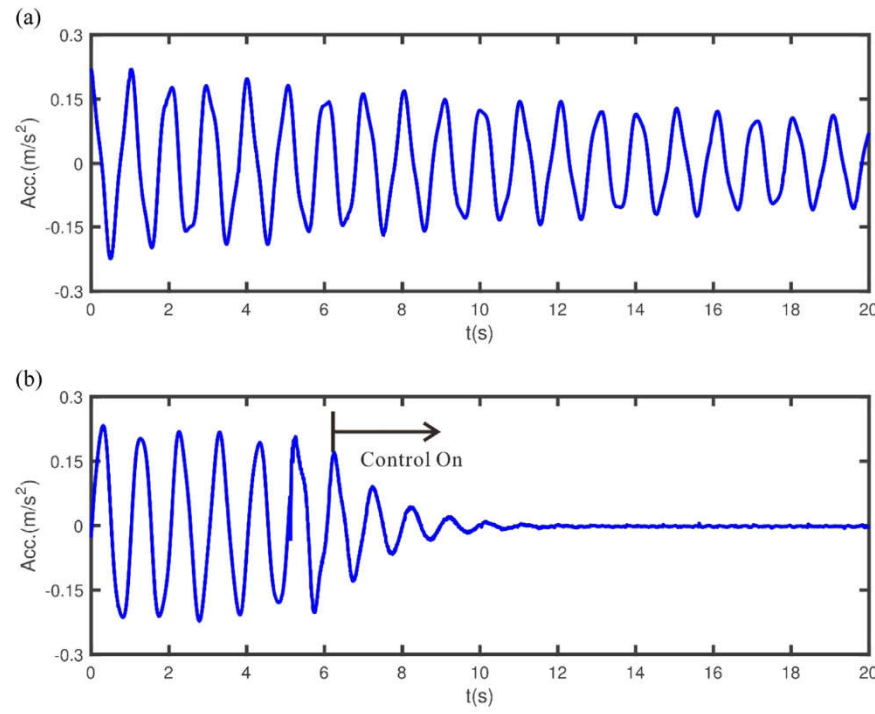


Fig. 12. Time history of acceleration for the first mode excitation: (a) Uncontrolled, (b) Controlled.

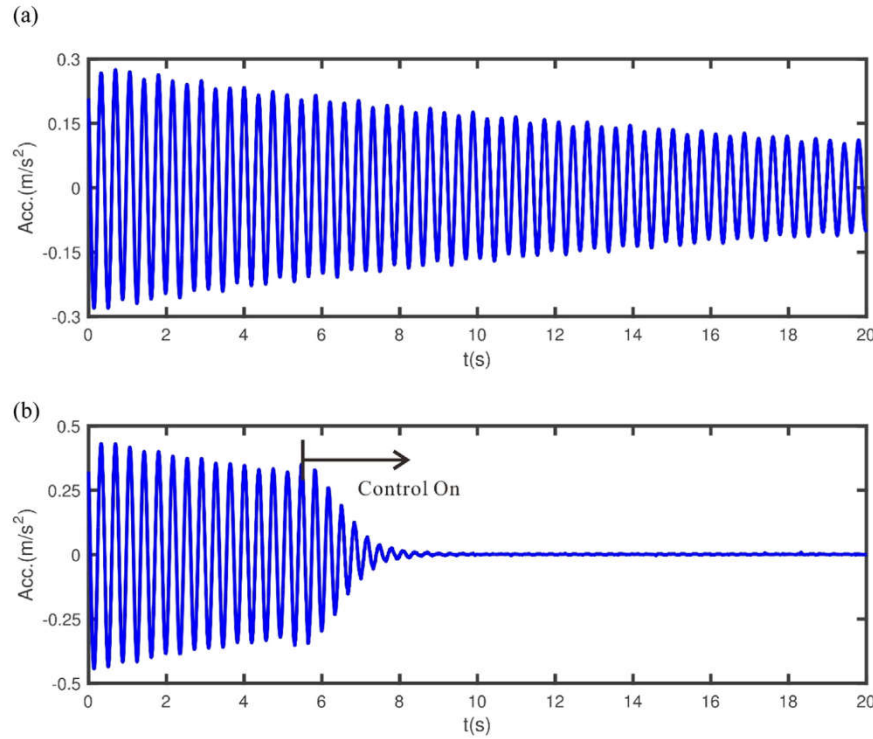


Fig. 13. Time history of acceleration for the second mode excitation: (a) Uncontrolled, (b) Controlled.

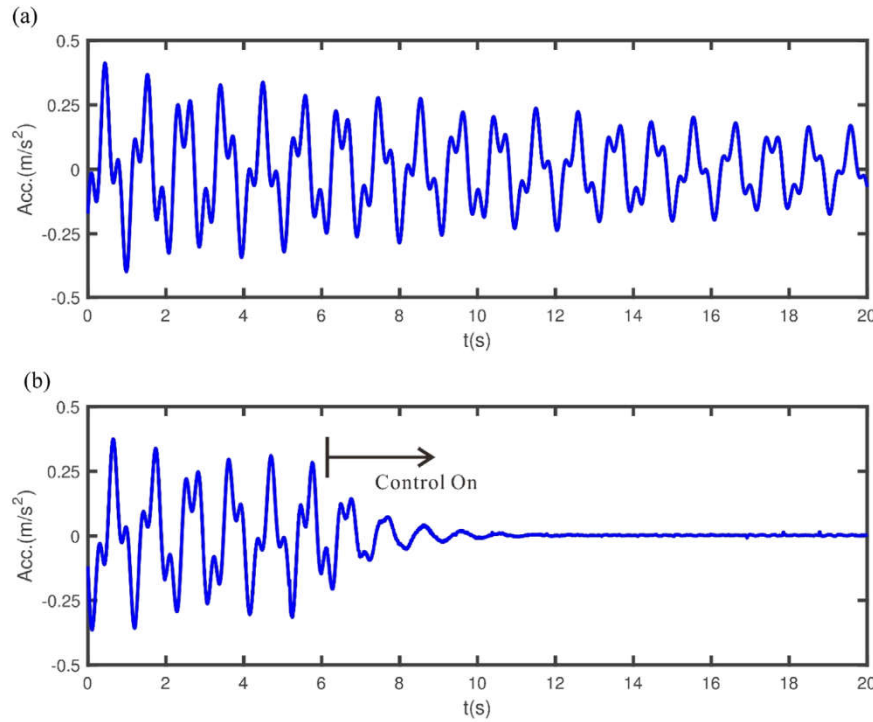


Fig. 14. Time history of acceleration for the two modes excitation: (a) Uncontrolled, (b) Controlled.

when the second natural mode of the structure was excited. Fig. 13(b) shows that the MMNAF control is also effective in suppressing the second natural mode. Fig. 14 shows the time history of acceleration when the two natural modes of the structure were excited. It can be seen from Fig. 14(b) that the MMNAF control is very effective in suppressing Multi-Modal vibrations.

6. Conclusions

In this study, the MMNAF control algorithm was proposed for the AMD system consisting of an AC servo motor and an accelerometer. The proposed MMNAF control generates the proper position for the active mass using the acceleration signal. Since the AC servo motor is operated by the velocity command mode, the additional control is necessary for the AC servo motor to follow the position command. The advantage of the MMNAF control is that it does not require an additional algorithm to compute velocity or displacement from the acceleration signal.

It was verified theoretically that the stability condition of a single NAF controller for the SDOF system is static and the NAF does not cause instability in the low frequency region unlike the PPF control.

It was also proven both theoretically and numerically that the MMNAF control is feasible if the gain matrix satisfies the stability condition in a MDOF system with a single AMD.

The test bed was built to identify the performance of the controller proposed in this study. It was proven experimentally that the proposed MMNAF control can successfully suppress multi natural modes of structures.

Acknowledgement

This research was supported by the Basic Science Research Program through the National Research Foundation of Korea (NRF) funded by the Ministry of Education (No. 2015R1D1A1A0905-7694).

References

- [1] R.J. McNamara, Tuned mass dampers for buildings, *J. Struct. Div.* 103 (9) (1977) 1785–1798.
- [2] D. Hrovat, P. Barak, M. Rabins, Semi-active versus passive or active tuned mass dampers for structural control, *J. Eng. Mech.* 109 (3) (1983) 691–705.
- [3] T. Pinkaew, Y. Fujino, Effectiveness of semi-active tuned mass dampers under harmonic excitation, *Eng. Struct.* 23 (2001) 850–856.
- [4] P.Y. Lin, LL. Chung, Semiaactive control of building structures with semiaactive tuned mass damper, *Comput.-Aided Civil. Infrastruct. Eng.* 20 (2005) 35–51.
- [5] N. Varadarajan, S. Nagarajaiah, Wind response control of building with variable stiffness tuned mass damper using empirical mode decomposition/Hilbert transform, *J. Eng. Mech.* 130 (4) (2004) 451–458.
- [6] S. Nagarajaiah, N. Varadarajan, Short time Fourier transform algorithm for wind response control of buildings with variable stiffness TMD, *Eng. Struct.* 27 (2005) 431–441.
- [7] S. Nagarajaiah, E. Sonmez, Structures with semiaactive variable stiffness single/multiple tuned mass dampers, *J. Struct. Eng.* 133 (1) (2007) 67–77.
- [8] G.L. Lin, C.C. Lin, B.C. Chen, T. Soong, Vibration control performance of tuned mass dampers with resettable variable stiffness, *Eng. Struct.* 83 (2015) 187–197.
- [9] M.K. Kwak, D.H. Yang, J.H. Shin, Active vibration control of structures using a semi-active dynamic absorber, *J. Noise Control Eng.* 63 (3) (2015) 287–299.
- [10] LL. Chung, R.C. Lin, T.T. Soong, A.M. Reinhard, Experimental study of active control for MDOF seismic structures, *J. Eng. Mech.* 115 (8) (1989) 1609–1627.
- [11] T. Kobori, N. Koshika, K. Yamada, Y. Ikeda, Seismic-response-controlled structure with active mass driver system. Part 1: design, *Earthq. Eng. Struct. Dyn.* 20 (1991) 133–149.
- [12] T. Kobori, N. Koshika, K. Yamada, Y. Ikeda, Seismic-response-controlled structure with active mass driver system. part 2: verification, *Earthq. Eng. Struct. Dyn.* 20 (1991) 151–166.
- [13] C.C. Chang, H.T.Y. Yang, Control of buildings using active tuned mass damper, *J. Eng. Mech.* 121 (3) (1995) 355–366.
- [14] S. Ankireddi, T.T. Yang, Simple ATMD control methodology for tall building subject to wind loads, *J. Struct. Eng.* 122 (1) (1996) 83–91.
- [15] H. Cao, A.M. Reinhard, T.T. Soong, Design of active mass damper for a tall TV tower in Nanjing China, *Eng. Struct.* 20 (3) (1998) 134–143.
- [16] C. Baoya, L. Chunxiang, Design of active tuned mass damper based on robust control, *Earthq. Eng. Struct. Dyn.* 29 (1) (2000) 127–137.
- [17] B. Samali, M. Al-Dawod, Performance of a five-storey benchmark model using active tuned mass damper and a fuzzy controller, *Eng. Struct.* 25 (2003) 1597–1610.
- [18] H. Cao, Q.S. Lin, New control strategies for active tuned mass damper systems, *Comput. Struct.* 82 (2004) 2341–2350.
- [19] A.P. Wang, Y.H. Lin, Vibration control of a tall building subjected to earthquake excitation, *J. Sound Vib.* 299 (2007) 757–773.
- [20] S.J. Dyke, B.F. Spencer, Jr., P. Quast, D.C. Kaspari, Jr., M.K. Sain, Implementation of an active mass driver using acceleration feedback control, *J. Micro-comput. Civil. Eng.* 11 (1996) 305–323.
- [21] I. Nishimura, T. Kobori, M. Sakamoto, N. Koshika, K. Sasaki, S. Ohnishi, Active tuned mass damper, *Smart Mater. Struct.* 4 (1) (1992) 306–311.
- [22] I. Nishimura, M. Sakamoto, T. Yamada, N. Koshika, T. Kobori, Acceleration feedback method applied to active-passive composite tuned mass damper, *J. Struct. Control* 1 (1–2) (1994) 103–116.
- [23] S.J. Dyke, B.F. Spencer, P. Quast, M.K. Sain, D.C. Kaspari, T.T. Soong, Acceleration feedback control of MDOF structures, *J. Eng. Mech.* 122 (9) (1996) 907–918.
- [24] E. Sim, W.W. Lee, Active vibration control of flexible structures with acceleration feedback, *J. Guid. Control* 16 (2) (1992) 413–415.
- [25] R.E. Christenson, B.F. Spencer, Jr., N. Hori, K. Seto, Coupled building control using acceleration feedback, *Comput.-Aided Civil. Infrastruct. Eng.* 18 (2003) 4–18.
- [26] S.N. Mahmoodi, M.J. Craft, S.C. Southward, M. Ahmadian, Active vibration control using optimized modified acceleration feedback with adaptive line enhancer for frequency tracking, *J. Sound Vib.* 330 (2011) 1300–1311.
- [27] J. Enriquez-Zarate, G. Silva-Navarro, H.F. Abundis-Fong, Active vibration suppression through positive acceleration feedback on a building-like structure: an experimental study, *Mech. Syst. Signal Process.* 72–73 (2016) 451–461.
- [28] T. Watanabe, K. Yoshida, T. Shimogou, T. Suzuki, M. Kageyama, A. Nohata, Reduced-order active vibration control for high-rise buildings, *JSME Int. J. Ser. C* 37 (3) (1994) 482–487.
- [29] J.L. Fanson, T.K. Caughey, Positive position feedback control for large space structures, *AIAA J.* 28 (4) (1987) 717–724.
- [30] <http://dl.mitsubisielctric.com/dl/fa/document/manual/servo/sh030052/sh030052b.pdf>.
- [31] <http://www.mitsubisielctric.com/fa/products/driv/servo/items/other/index.html>.
- [32] <http://www.jewellinstruments.com/linear-angular-accelerometers>.
- [33] <https://www.dspace.com/en/pub/home/products/hw/singbord/ds1104.cfm>.